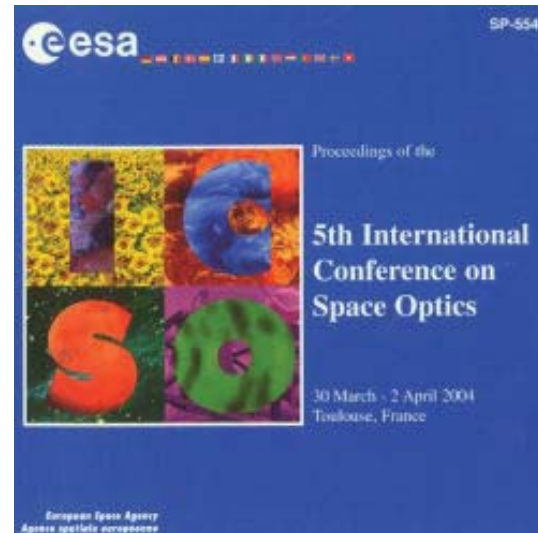


International Conference on Space Optics—ICSO 2004

Toulouse, France

30 March–2 April 2004

Edited by Josiane Costeraste and Errico Armandillo



Cryogenic optical testing of sic mirrors for ASTRO-F and C/SiC composite mirrors for SPICA

Hidehiro Kaneda, Takao Nakagawa, Keigo Enya, Takashi Onaka



CRYOGENIC OPTICAL TESTING OF SiC MIRRORS FOR ASTRO-F AND C/SiC COMPOSITE MIRRORS FOR SPICA

Hidehiro Kaneda⁽¹⁾, Takao Nakagawa⁽²⁾, Keigo Enya⁽³⁾, Takashi Onaka⁽⁴⁾

⁽¹⁾ ISAS / JAXA, Yoshino-dai 3-1-1, Sagamihara, Kanagawa 229-8510, Japan, E-mail: kaneda@ir.isas.jaxa.jp

⁽²⁾ ISAS / JAXA, Yoshino-dai 3-1-1, Sagamihara, Kanagawa 229-8510, Japan, E-mail: nakagawa@ir.isas.jaxa.jp

⁽³⁾ ISAS / JAXA, Yoshino-dai 3-1-1, Sagamihara, Kanagawa 229-8510, Japan, E-mail: enya@ir.isas.jaxa.jp

⁽⁴⁾ Department of Astronomy, University of Tokyo, Hongo 7-3-1, Bunkyo-ku, Tokyo 113-0033, Japan, E-mail: onaka@astron.s.u-tokyo.ac.jp

ABSTRACT

Light-weight mirrors are developed for two Japanese infrared astronomical missions, ASTRO-F and SPICA. ASTRO-F is scheduled for launch in 2005, while the target year for launch of SPICA is 2010. The mirrors of the ASTRO-F telescope are made of a sandwich-type silicon carbide (SiC) material, comprising porous core and CVD coat of SiC on the surface. Cryogenic measurements of the ASTRO-F primary mirror and telescope assembly were performed extensively. As for the SPICA telescope, which has an aperture of 3.5-m diameter, carbon-fiber-reinforced SiC (C/SiC composite), as well as SiC, is one of the promising candidates for mirror material. C/SiC composite spherical test mirrors of 160-mm diameter has recently been manufactured and tested. This paper presents the experimental results of the cryogenic performance obtained for the sandwich-type SiC mirrors and the C/SiC composite mirrors.

1. INTRODUCTION

The first Japanese infrared astronomical satellite, ASTRO-F, which is scheduled for launch in the summer of 2005 [1], is designed to make survey observations from near-infrared to far-infrared (2-200 microns) region with two focal-plane scientific instruments [2] [3]. The ASTRO-F telescope forms an F/6 Ritchey-Chretien system with a primary mirror of 700 mm in diameter [4] [5]. The whole telescope system is cooled down to 5.8 K with a combined use of super-fluid liquid helium and mechanical coolers in order to suppress the thermal background. Nearly diffraction-limited performance in the near-infrared region is required for the ASTRO-F telescope system to achieve faint-object detections. The telescope assembly, which incorporates the primary and secondary mirrors, baffles, and support structures, must retain the alignment after launch vibration as well as cool-down. Additionally, stringent telescope mass requirements call for the use of lightweight mirror technologies for the ASTRO-F telescope. Hence, the

sandwich-type SiC material, consisting of a light porous SiC substrate and a dense CVD coat of SiC, is employed for the ASTRO-F primary and secondary mirrors. Porous core SiC plays an important role in realizing light weight and easy machining, while hard CVD SiC enables us to figure a mirror surface very accurately.

The project for the Space Infrared Telescope for Cosmology and Astrophysics (SPICA) mission has started, following the ASTRO-F project [6] [7]. SPICA is an observatory-type mission with a 3.5-m telescope that will be optimized for mid- and far-infrared observations. The target year for launch of SPICA is 2010. The telescope is to be launched at an ambient temperature and is to be cooled in orbit to 4.5 K by a mechanical cooler system with assistance of effective radiation cooling. The resources of the mission require that the total weight of the telescope system must be lighter than 700 kg. The telescope system also has a requirement to be diffraction-limited at 5 μm at 4.5 K. Currently, we are investigating two candidate materials for the monolithic primary mirror: silicon carbide (SiC) and carbon-fiber-reinforced SiC (C/SiC composite) [8]. C/SiC composite spherical mirrors of 160-mm diameter have recently been fabricated, and the surface figure and the surface roughness at low temperatures have been measured. The tested mirror employs a new type of C/SiC composite material developed for large light-weight mirrors in future, which has larger mechanical strength than normal C/SiC. The test results show promising applicability of the C/SiC composite material to the SPICA telescope mirrors

This paper reports the results of the cryogenic optical testing so far obtained for the SiC mirrors and the C/SiC composite mirrors, and refers to a trade-off between SiC and C/SiC composite materials.

2. SiC AND C/SiC MIRRORS

Basic material properties of CVD SiC and a C/SiC composite are displayed in table 1, together with those of

other representative mirror materials. SiC and a C/SiC composite have an excellent thermal conductivity compared to Zerodur, and a smaller specific heat and CTE than those of metals such as beryllium. Particularly, SiC and a C/SiC composite have a large Young's modulus and thus can be polished to a high precision. Furthermore, SiC and a C/SiC composite is a very tough material against hitting of high-energy particles, which is also suitable to space applications.

Table 1. Material properties at a room temperature

	units	C/SiC	CVD SiC	Be	Zerodur
Young's modulus	GPa	320	448	303	89
Density	g/cm ³	2.65	3.21	1.85	2.53
CTE	ppm/K	2.3	2.6	11.4	0.02
Conductivity	W/m/K	125	240	180	1.6
Specific heat	J/kg/K		710	1925	820
Bending strength	MPa	175	785		80

Pictures of the ASTRO-F flight-model primary mirror are displayed in Figs.1b and 1c. Manufacturing process of the sandwich-type SiC mirrors is as follows: a sintered porous SiC blank is machined to an open-back structure with thickness of 3 mm both for a surface and backside ribs. The porous substrate is then coated with CVD SiC of 0.5 mm thickness on both the front and rear surfaces, the total thickness of SiC being 4 mm. After grinding and polishing, the front surface is coated with Au and ZnS; the former coating increases the reflectivity in the infrared region, while the latter makes the strong surface to allow cleaning.

The primary mirror weighs about 11 kg, which corresponds to the areal density of 28 kg/m². The rim of the mirror surface is black-painted in order to reduce the additional diffraction and scattering of photons. The primary mirror is supported by three bipod flexures made of titanium alloy, which are fixed to the optical aluminum base-plate. The flexures are attached to the SiC mirror through the support structure made of super-invar (Fig.1c). The super-invar support structures, which have been pre-cooled twice down to a liquid nitrogen temperature, are glued to the rear holes.

Prior to the manufacture of the ASTRO-F mirrors, three pieces of small-size sandwich-type SiC mirrors (160 mm in diameter) with a similar structure to the ASTRO-F mirror have been fabricated (Figs2a and 2b) and the mirror figures at cryogenic temperatures have been measured by an interferometer [9]. All of them have the same design of the spherical F/3.0, but have undergone processing with slightly different parameters. The test results on the final product convinced us of favorable applicability of this kind of SiC material to the ASTRO-F telescope mirrors.

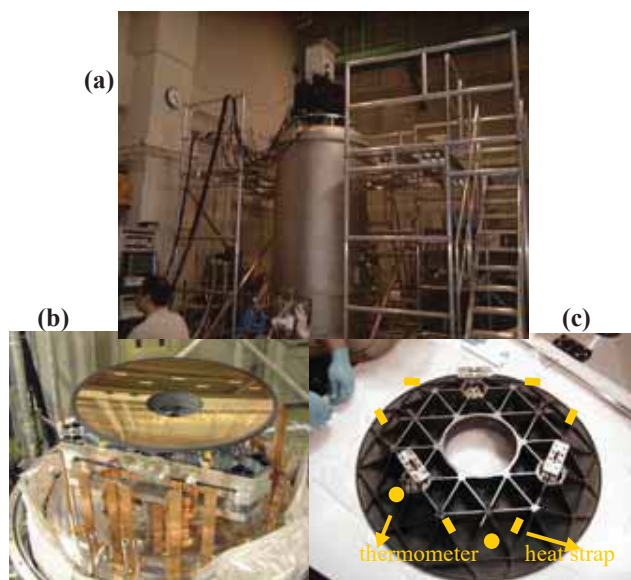


Fig.1. (a) Test chamber facility, (b) ASTRO-F primary mirror mounted on the cold stage inside the chamber, (c) rear-side structure of the primary mirror.

Extension of our heritages from the ASTRO-F sandwich-type SiC mirrors to the SPICA telescope mirrors encounters a great difficulty: a large CVD furnace required for 3.5-m diameter mirrors is currently unavailable. A brittle nature of the SiC material might become more serious as the size of the mirror is getting larger. One possibility to overcome the former difficulty is a brazed SiC mirror adopted for the Herschel Space Observatory, and another for the latter is a C/SiC composite mirror. The C/SiC composite material has the following advantages over SiC: (1) high fracture toughness, (2) good machinability, (3) established joint technology, and (4) low cost. Hence, a C/SiC composite is very promising new material for light-weight mirrors. However, existing C/SiC composite material is not strong enough as compared to SiC (table 1). Furthermore, the composite nature of C/SiC may require careful polishing processes. For application to future large-telescope missions, Mitsubishi Electric Corporation has recently improved C/SiC composite material.

Cryogenic properties of C/SiC composite material are far from complete understanding since a C/SiC composite itself is a rather new material, and thus fundamental understanding of cryogenic optical performance of the C/SiC composite mirror is the most important issue in its application to the SPICA telescope mirrors. As the first step, small-size C/SiC composite sample mirrors (160 mm in diameter) have been fabricated (Figs.2c and 2d) and tested at low temperatures. Three segments made of C/C composite material are bonded together at the stage of Si infiltration into carbon matrices; the joint I/F lines are schematically indicated in dotted lines in Fig.2d

Hence, the measurements enable us to confirm the applicability of the joint technology to cooled mirrors and to evaluate the effect of small CTE differences among the three segments on the cryogenic deformation. Grinding and polishing are performed on the bare surface of the bonded C/SiC composite blank without application of any surface coat, e.g. CVD coating, to form a F/6.0 spherical mirror. The mirror has 5 mm thickness for the surface and 3 mm thickness for the backside ribs. Cryogenic measurements of the surface figure and the surface roughness of this sample mirror gave us reasonable promise for further development of this type of C/SiC composite mirrors

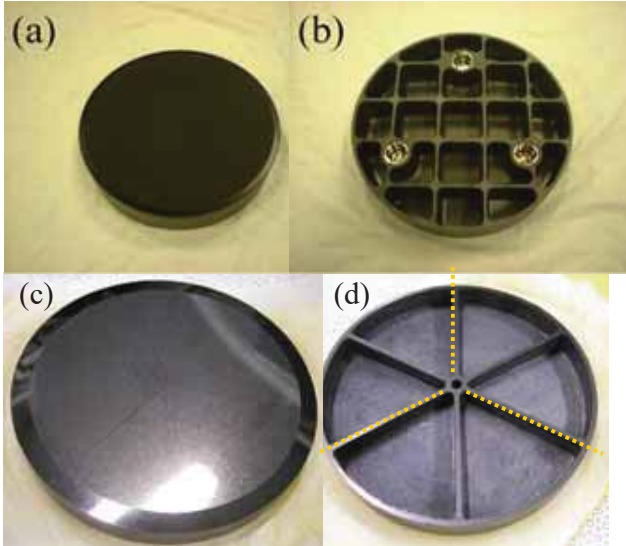


Fig.2. (a) 160-mm-diameter SiC mirror and (b) its rear-side structure. (c) 160-mm-diameter C/SiC composite mirror, and (d) its rear-side structure.

3. MEASUREMENTS

3.1 160-mm test mirrors

Fig.3 shows the setup of the cryogenic optical measurements for the 160-mm-diameter mirrors of the sandwich-type SiC or the C/SiC composite material. The mirror is hung by a stainless steel belt in a liquid-helium chamber to avoid extra stress for the support. The changes in the surface figure are directly measured through the vacuum-sealing entrance window from outside the chamber by a ZYGO GPIxp interferometer. The alignment between the mirror and the measurement system is adjusted by the X/Y and Z stages upon which the interferometer is placed. The measurement system and the chamber are set up on a vibration-free table. Three thermal straps are attached to the backside ribs of the mirror. A thermometer is also attached to the backside rib to monitor the temperature of the mirror itself. The lowest temperature of the mirror reached in every measurement ranges from 6 K to 15 K. The

measurements of the surface figure were performed while the mirror was being warmed up, where the stable measurements were possible.

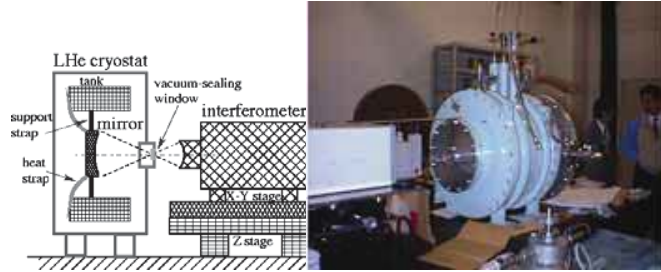


Fig.3. Setup of cryogenic optical measurements of the small-size SiC or C/SiC composite mirrors.

3.2 ASTRO-F primary mirror

Fig.1a shows the test chamber facility for optical measurements of large-aperture (<800 mm) mirrors and telescopes at a liquid-helium temperature. The whole facility is placed inside the clean booth; the chamber has a height of 3.4 m, and the scaffolding with a similar height surrounds the chamber that enables us to reach the upper side of the chamber. The measurement system which consists of a ZYGO GPIxp interferometer and a combination of three-axis shift and two sets of two-axis tilt adjustment stages is placed upon the top plate of the chamber. During the optical measurements, the whole system is being sustained by four vibration-free supports, which have a capability of auto-leveling adjustment within accuracy of 0.25 mm. There are four windows to observe the inside of the chamber, one on the top, one on the bottom, and two on the side wall in the X/Y directions. Each window is closed by a cold shutter during the cooling down which is thermally connected to the 80 K shroud. There are X/Y shift and two-axis tilt adjustment stages inside the chamber, which can be driven at a liquid-helium temperature.

Fig.4a displays a schematic view of the cryogenic optical measurements of the primary surface. The primary mirror is mounted onto the top plate of the tilt adjustment stage via the triangular base-plate in the chamber (Fig.1b). The surface figure of the mirror is measured from outside the chamber by the interferometer through the null lens and the entrance window. The alignment between the optical axes of the mirror and the measurement system is monitored by the alignment telescope; first the alignment telescope is set up on the bottom plate of the chamber and the alignment between the primary mirror and the entrance window is adjusted by the inner adjustment stages, and then, the alignment telescope is put on the top plate of the chamber and the alignment between the entrance window and the null lens is adjusted by the upper adjustment stages. In installing

the null lens, the distance between the primary mirror and the null lens is measured by the absolute distance meter and adjusted by the upper Z-axis adjustment stage.

Six thermal straps and two thermometers attached to the backside ribs of the primary mirror (Fig.1c). The mechanical connection between the base-plate and the cold adjustment stage was set to be loose in order to avoid extra stress on the mirror. The cryogenic measurements of the primary mirror were performed twice. The lowest temperatures of the mirror reached in the two measurements were about 10 K, which was slightly above the expected operating temperature (5.8 K) of the ASTRO-F telescope. The difference in the temperature between the two thermometers attached to the primary mirror was very small (<200 mK) at low temperatures, indicating good thermal conductivity of the SiC material even at cryogenic temperatures.

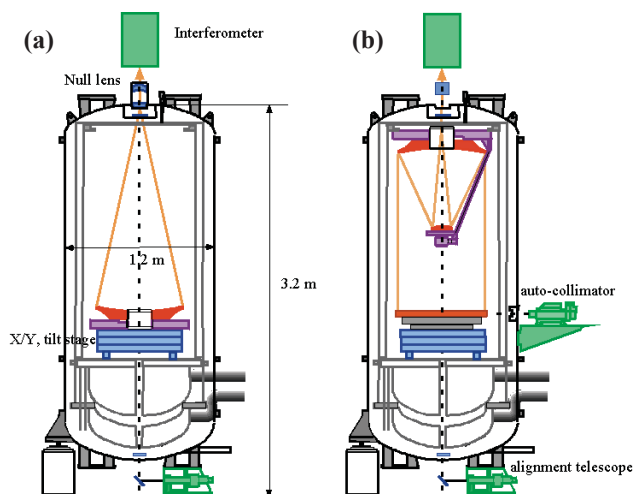


Fig.4. Schematic views of optical measurements of (a) primary mirror, and (b) telescope assembly.

3.2 ASTRO-F telescope system

After the testing of the primary mirror, the secondary mirror and the telescope truss were integrated into the flight-model telescope system. The manufacturing process of the secondary mirror is the same as that of the primary mirror except for the size and the curvature. The secondary mirror is supported by titanium alloy flexures in a similar way to the primary mirror. The telescope truss is made of beryllium. Before cooling, 0 dB random vibration tests were conducted for the telescope assembly (Fig.5a). By interferometric measurements before and after the vibration test, we confirmed that the wave-front error did not change significantly and thus the telescope retained the alignment even after launch vibration. The telescope was then installed into the chamber (Fig.5b) and tested under the configuration shown in Fig.4b. The

telescope assembly is suspended from the top ring of the 4 K innermost thermal shroud, while the reflecting flat mirror is placed on the inner adjustment stages through the Hindle mounting technique (Fig.10a). The reflecting flat mirror is made of fused silica with a diameter of 750 mm, manufactured by SAGEM. Since fused silica has low thermal conductivity, we had to cool the flat mirror using 64 thermal straps, which were attached to the rear surface of the mirror. The flat mirror has two reflecting flat surfaces in the X/Y directions on the lateral side, which are used to monitor the tilt angle of the flat mirror by auto-collimators from outside the chamber.

The mechanical connection between the telescope and the 4 K top ring was set to be loose to avoid extra stress on the telescope due to the thermal contraction of the top ring. The lowest temperatures thus achieved were 13 K for the primary mirror, 14 K for the secondary mirror, and 17 K for the flat mirror. The difference in the temperature between the primary and the secondary mirror was at most 2 K at low temperatures.

The ASTRO-F telescope has a one-axis movement mechanism of the secondary mirror for focus adjustment, so that the distance between the primary and the secondary mirrors is adjustable within a stroke of 0.80 mm and a resolution of 0.47 μm . The focus adjustment was conducted at a cryogenic temperature during the optical measurements of the mirror surfaces, which confirmed that the focus of the telescope was well adjustable with the designed stroke and resolution.

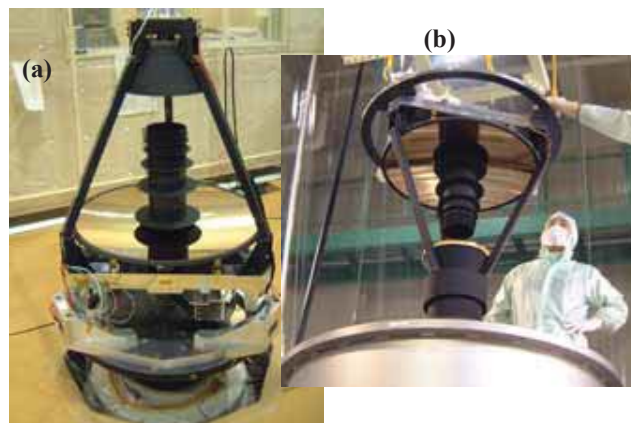


Fig.5. ASTRO-F flight-model telescope during (a) vibration test and (b) installation into the chamber.

4. RESULTS

4.1 160-mm SiC mirrors

The surface figures measured for the 160-mm SiC mirrors at a room and a cryogenic temperature are shown in Fig.6. Here and hereafter, the surface figure is shown

after subtraction of the ideal surface figure, and is given as half a wave-front error measured by the interferometer. A conspicuous local minimum is observed in the central region for every mirror figure, which is attributed to additional spherical aberrations due to the presence of the vacuum-sealing window along the optical path.

As clearly seen in Fig.6, the cryogenic performance has been improved considerably from the second to the third mirror owing to the optimizations of the manufacturing process. Details on the differences in the manufacturing process among the three SiC mirrors and their effects on the measured cryogenic performances are described in [9]. Major differences between the second and the third SiC mirror are as follows: the CVD coating was made only once for the second mirror and the bottoms of the three interface holes on the rear surface (Fig.2b) have been left uncoated with CVD to keep the reference surface of the core blank. For the third SiC mirror, the CVD coating was conducted twice so that coating over all the front and rear surfaces was achieved and the top SiC layer on the mirror surface was removed completely during the grinding process. Since the phase of the peaks seen in the second mirror exactly corresponds to that of the above non-CVD-coated holes, the deformation may originate from bi-metal effects due to a slight difference in the CTE between the porous and CVD SiC. On the other hand, the surface figure of the third SiC mirror changed very little under temperature variations. Hence, the importance of the SiC-CVD coating over the whole surface of the porous core has been confirmed.

As for the second and the third SiC mirrors, the surface figure error for every measurement is plotted against the temperature in units of λ in Fig.11. Here and hereafter, λ is 632.8 nm of He-Ne laser. The figure error relative to the initial surface figure measured before the cooling is also plotted, which is lying on the lower side for each mirror. The third SiC mirror shows the smallest figure error among the three mirrors at 6 K, although the figure error at 300 K is larger than that of the second mirror. The differences from the initial surface figures of the second and the third SiC mirror around 300 K are as small as 0.01 λ rms, which supports no significant hysteresis produced by the cooling cycle considering the systematic error due to the subtraction of the two data files. From Figs.6 and 11, it can be concluded that the surface figure of the third mirror at 6 K is the same as that at 300 K within the measurement uncertainties; there may be a possible transient deformation around 180 K for the third mirror. This distortion could reflect a material property peculiar to the combination of the porous SiC and CVD SiC. However, it is still as small as 0.03 λ rms and disappears at lower temperatures.

By using the third SiC mirror that showed the best cryogenic performance, the effects of the support

structures have been investigated. For their attachment to the rear holes (Fig.2b), three kinds of cryogenic adhesive agents, Stycast 2850FT, EC2216, and EP007, were used separately at three attaching points of the mirror, all of which had been confirmed to have a sufficient adhesive strength at a liquid nitrogen temperature. The super-invar support structures were pre-cooled twice down to a liquid nitrogen temperature before the attachment. As a result of optical testing, Stycast 2850FT yielded the smallest deformation at cryogenic temperatures among the three glues, although it showed non-negligible hysteresis upon return to a room temperature. Hence, Stycast 2850FT was concluded to be the best choice for the ASTRO-F telescope.

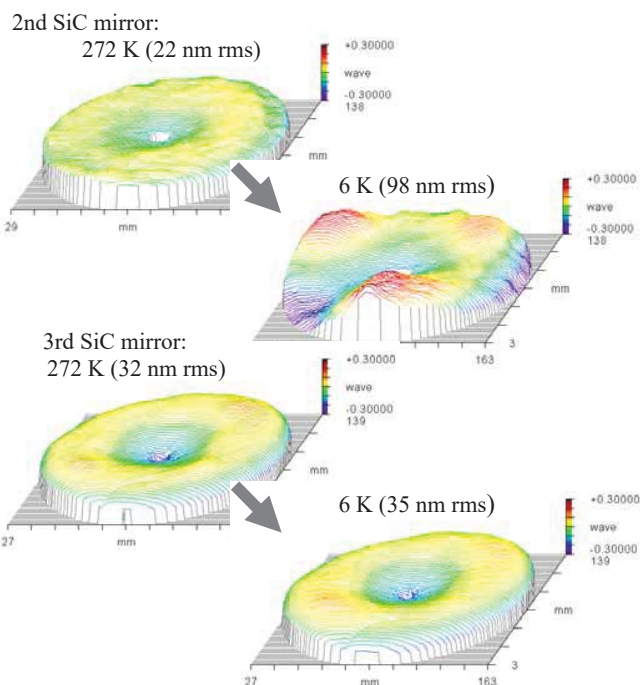


Fig.6. Changes of surface figures for the second (upper) and the third SiC mirror (lower) with temperature.

4.2 ASTRO-F primary mirror

The surface figures measured for the primary mirror at a room and a cryogenic temperature are shown in Fig.7. Three-phase rotationally-symmetrical local maxima are clearly observed at a room temperature (Fig.7a). The phase of the peaks corresponds to that of the flexures and the support structures (Fig.1c). Before the installation into the chamber, such maxima had not been observed under the configuration that the primary mirror was placed on the whole rear surface without any support structures. Therefore, we concluded that the resultant three-phase deformation originated from gravitational effects. The surface figure error of the primary mirror without the support structures is 48 nm rms, which is

much smaller than that of the mirror with the support structures, 130 nm rms, and thus degradation in the mirror figure due to the gravity is quite serious. A model prediction shows a fair agreement with the observed deformation.

As seen in Fig.7b, the surface figure changed appreciably from 287 K to 10 K. Trefoil deformation was clearly observed at cryogenic temperatures in the same phase as the gravitational deformation. Judging from the result that the surface figure of the 160 mm SiC mirror showed very little cryogenic deformation, the main fraction of the cryogenic deformation is reasonably considered to be due to the thermal contraction of the base-plate; the flexures cannot absorb entire difference in CTE between the SiC primary mirror and the aluminum base-plate. Such deformation has been predicted to some extent by a model calculation, however the model cannot reproduce exact figure such as sudden depressions and sharp ridges. The former may be associated with the attachment of the thermal straps, which further degrade the surface figure of the primary mirror at cryogenic temperatures.

The primary mirror showed serious permanent deformation upon return to a room temperature. Fig.8a displays the surface figure that was measured at a room temperature after the first cooling and shown after subtraction of the mirror figure measured at a similar temperature before the cooling. From Fig.8a, the permanent change of the mirror surface that occurred by the first cooling cycle consists of two components: dimples at the positions of the support structures and turn-ups around the circumference. The phase of the latter component is the same with that of the depression observed at cryogenic temperatures, which corresponds to that of the thermal straps at the backside ribs. From the positional coincidences, it is reasonable to consider that the three-phase dimples are due to residual deformation of the super-invar support structures, while the turn-up deformation is related to plastic deformation of the structures of the heat anchors made of copper; the copper structures have not been pre-cooled before attachment to the backside ribs, although the super-invar support structures were pre-cooled twice. As described later, the permanent deformation of the support structures is well explained by the anomalous behavior of super-invar metal at low temperatures.

Since the hysteresis was detected unexpectedly, the primary mirror was re-cooled and the mirror figure was measured again before and after the cooling. As seen in Fig.8b, the mirror surface did not show any further hysteresis significantly after the second cooling cycle. Hence, the hysteresis that was observed just after the first cooling degraded the surface figure of the primary mirror seriously. Since it was confirmed that the telescope system still barely met the requirements (see next

section), we decided not to make further work on it.

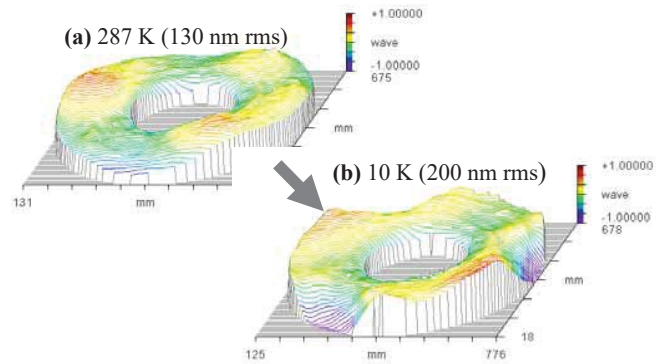


Fig.7. Changes of surface figure for the primary mirror with temperature. Both are shown in the same scale.

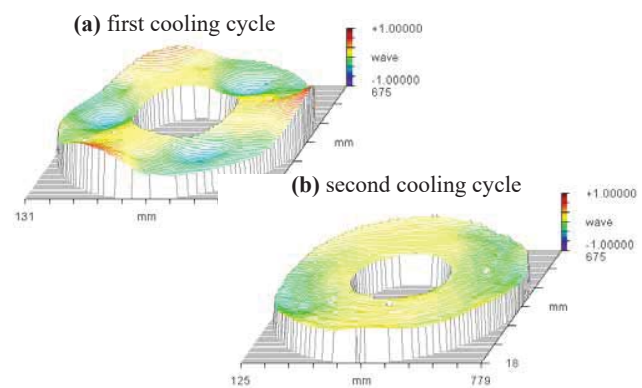


Fig.8. Difference in surface figure of the primary mirror between before and after (a) the first cooling cycle and (b) the second cooling cycle.

4.3 ASTRO-F telescope system

The wave-front errors measured for the telescope system at a room and a cryogenic temperature are shown in Fig.9. In this case, the rms values indicated together are evaluated by a quarter of the wave-front errors measured by the interferometer. We have to be aware that, if the flat mirror has an ideal flat surface, the total wave-front error of the telescope itself is equal to half the measured wave-front error, and thus the rms value evaluated by a quarter of the error corresponds to the surface figure error of a combination of the primary and the secondary mirror. The phase of the figure in Fig.9 should be rotated by 30 degrees to match with that of the figures in Figs.7 and 8. The shade area seen in Fig.9 is attributed to the baffle of the secondary mirror and the telescope truss.

In comparison between Fig.7a and Fig.9a, the three-phase local enhancements at the support structures observed in the measurement of the primary mirror alone are replaced by the local depressions at the same

positions in the measurement of the telescope assembly. This is because the gravity force relative to the primary mirror surface works in reverse. In consequence of the cryogenic measurements, the surface figure exhibited trefoil deformation similarly to the case of the primary mirror alone except for the local minima at the support structures that are again gravitational distortions. The ridges are more clearly seen in the figure due to the presence of the local minima. In addition to the similarity in the surface figure, the surface figure error itself at cryogenic temperatures shows a similar value to that of the primary mirror alone. Hence, we can conclude that a substantial fraction of the cryogenic deformation of the telescope system is due to the deformation of the primary mirror and almost no misalignment between the primary and the secondary mirror was generated by the cooling. It implies that the cryogenic deformation of the secondary mirror is negligible and uniformity in the thermal contraction of the telescope truss is quite well.

The flat mirror can exhibit significant deformation at cryogenic temperatures and thus may affect the above evaluation. Therefore, we attempted the extraction of the surface figure of the flat mirror itself by independently moving the flat mirror in the X/Y directions with the inner adjustment stage. Every time the flat mirror is shifted, the tilt angle of the flat mirror is monitored by the auto-collimator from outside the chamber and the observed tilt was taken into account in the following calculation. We differentiated the surface figure using the two sets of wave-front data measured before and after a 40-mm shift of the flat mirror in the X or Y direction. Two differential figures obtained from the shifts of the flat mirror in the X/Y directions are then averaged. The differential figure thus derived is shown in Fig.10b by Zernike polynomial approximation. Details of the methodology are described in [10].

One particular problem to be concerned here is whether or not the shift of the flat mirror can generate misalignment between the telescope and the flat mirror as well as that between the primary and the secondary mirror because the small change in the center of gravity can cause the significant bending of the 4 K thermal shroud and thus that of the telescope truss. Owing to the capability of the auto-leveling adjustment of the vibration-free supports, however, the chamber cannot be tilted at an angle of more than 2 arcmin and therefore we concluded that there was no significant misalignment introduced by the shift of the flat mirror. The surface figure error of the flat mirror at a cryogenic temperature is estimated to be as small as 41 nm. As a result, we can safely neglect the contribution of the distortion of the flat mirror to the total wave-front errors of the telescope. Since the surface figure error of the flat mirror at a room temperature is only 7.6 nm, the change in the surface figure at cryogenic temperatures is yet significant.

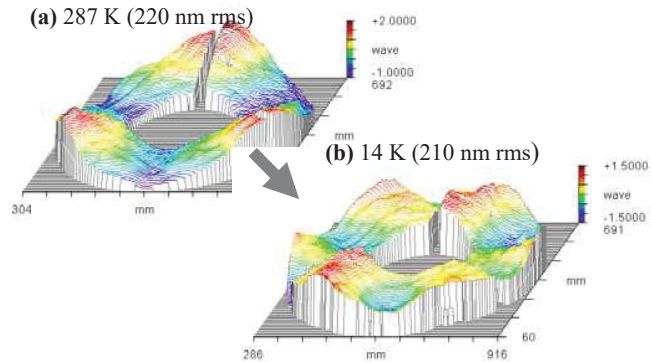


Fig.9. Changes of surface figure (half the total wavefront error) for the telescope assembly with temperature.

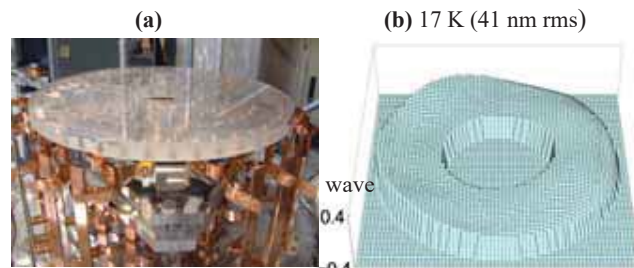


Fig.10. (a) Reflecting flat mirror mounted on the stage inside the chamber. (b) Cryogenic deformation of the flat mirror.

3.4 160-mm C/SiC composite mirror

The surface figure was measured for the 160 mm C/SiC composite mirror at a room and a cryogenic temperature. The obtained figure error for every measurement is plotted against temperatures in Fig.11. The figure error relative to the initial surface figure measured before cooling is also plotted. As seen in Fig.11, there are no dramatic changes of the surface figure error toward cryogenic temperatures. However, significant permanent deformation was produced by the cooling cycle; the difference from the initial surface figure around 300 K is as large as $0.15 \lambda_{rms}$. An origin of the observed large-scale permanent deformation is still under investigation; it does not seem to correlate with the pattern of the three segments. Apart from the large-scale structure, local depressions of $\lambda/20$ in depth appeared along the joint lines of the three segments, where the separate C/C composite materials had been bonded together at the stage of the Si infiltration (Fig.2). The C/SiC composite mirror was then re-cooled and the surface figure was measured again; the mirror surface did not show any further hysteresis significantly before and after the cooling. Obviously, the initial surface figure error of the tested sample mirror is rather large, and thus measurement sensitivity for the surface figure is limited

by its poor accuracy. Hence, further polish of the mirror to a higher precision would be inevitable as a next step, and therefore polishing technology of bare C/SiC surfaces should be established. Alternatively, polishability of C/SiC surfaces might be enhanced by application of some coating technique.

Degradation of the surface roughness by the carbon fibers at low temperatures is another major concern for this type of composite mirrors. So far, by using the flat mirror of the C/SiC composite material, microscopic measurements of the surface by using a ZYGO Newview interferometer, as well as speckle measurements by scattering rays of light incident on the mirror, have been performed at a room and a liquid-nitrogen temperature. Preliminary results of the measurements showed no significant degradation of the surface roughness toward a liquid-nitrogen temperature as compared with the initial surface roughness of about 20 nm rms for the tested flat mirror. Details of these cryogenic tests of the C/SiC composite mirror will be reported in a separate paper.

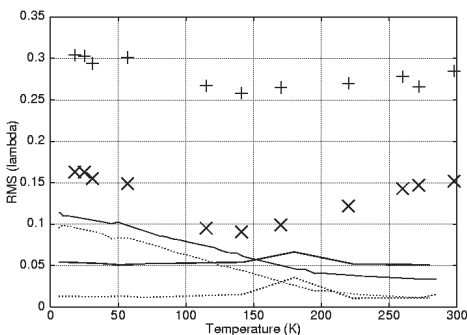


Fig.11. Plots of surface figure error for the C/SiC composite mirror against temperature (pluses). Figure error relative to the initial surface figure measured before the cooling is also plotted (crosses). In addition, figure errors for the second and the third 160-mm SiC mirror are shown in a dotted and a solid line, respectively.

4. CURRENT STATUS & FUTURE PLAN

After the cryogenic optical testing of the ASTRO-F telescope, the telescope system integrated with the flight-model focal-plane instruments was installed into the flight-model cryostat, and 0 dB random and shock vibration tests were conducted at a liquid-helium temperature. As a result, the cryogenic vibration tests gave some damage to the support structures of the primary mirror, where the super-invar structures were detached from the SiC rear holes. This failure has delayed the schedule of ASTRO-F by 1.5 years, which was supposed to be launched in February 2003. We have concluded that the detachment of the support structures is exclusively due to large CTE mismatch between super-invar and SiC. We had been unaware that

super-invar undergoes the Martensitic transformation at low temperatures; super-invar, once cooled down below 200 K, comes to behave like metal with rather large CTE, which produces fatal thermal stress for the support structures at cryogenic temperatures. Currently, the refurbishment of the telescope is underway, the super-invar support structures being replaced by normal invar ones which have been confirmed to show no transformation at cryogenic temperatures. The cryogenic optical testing will be again performed for the newly-integrated telescope in May-June 2004.

For the SPICA project, we are currently searching for two possibilities for the primary mirror: sintered SiC with the brazing technique and the C/SiC composite. Next year, bread-board model (BBM) mirrors of about 700 mm in diameter will be manufactured for both materials and by using the above telescope chamber facility, each tested at cryogenic temperatures in a combination of appropriate support mechanisms. As for the C/SiC composite mirror, prior to the BBM mirrors, two kinds of 160 mm C/SiC composite mirrors will be tested again at cryogenic temperatures; one will have a bare C/SiC surface polished to a high precision, and the other will have a mirror surface processed with some coating technique.

ACKNOWLEDGMENTS

We are indebted to all the members of the ASTRO-F project and the SPICA working group. Particularly, we thank S. Miura, Y. Numao, Y. Sugiyama, R. Yamashiro, and other staffs in NIKON corporation for their continuous efforts in manufacturing the SiC mirrors and appropriate guidance in the optical measurements. We are also deeply grateful to T. Ozaki, T. Oshima, and other staffs in Mitsubishi Electric Corporation for their great efforts in developing the C/SiC composite mirrors.

REFERENCES

1. Shibai H., *Proc. SPIE* 4850, 162, 2003.
2. Takahashi H., et al., *Proc. SPIE* 4013, 47, 2000.
3. Wada T., *Proc. SPIE* 4850, 179, 2003.
4. Kaneda H., Onaka, T., Yamashiro R., and Nakagawa, T., *Proc. SPIE* 4850, 230, 2003.
5. Onaka T., Sugiyama Y., and Miura S., *Proc. SPIE* 3354, 900, 1998.
6. Matsumoto T., *Proc. SPIE* 4850, 12, 2003.
7. Nakagawa T., and SPICA working group, *ESA SP-460*, 475, 2001.
8. Onaka T., et al., in this volume, 2004.
9. Kaneda H., Onaka, T., Kawada, M., and Murakami, H., *Appl. Opt.* 42, 708, 2003.
10. Sugiyama Y., Yamashiro R., Numao, Y., Onaka T., Kaneda H., and Nakagawa T., *27th Optics Symposium Proceedings, The Optical Society of Japan*, 2002.